Dynamic field on 40-MeV μ^+ traversing magnetized iron

J. M. Brennan, N. Benczer-Koller, and M. Hass*
Rutgers University, New Brunswick, New Jersey 08903

W. J. Kossler and J. Lindemuth
The College of William and Mary, Williamsburg, Virginia 23186

A. T. Fiory, D. E. Murnick, and R. P. Minnich
Bell Laboratories, Murray Hill, New Jersey 07974

W. F. Lankford
George Mason University, Fairfax, Virginia 22030

C. E. Stronach
Virginia State College, Petersburg, Virginia 23803

(Received 1 February 1978)

Previous experiments have demonstrated the existence of large dynamic magnetic fields that act on positive heavy ions traversing magnetized iron. These studies have been extended to the limit of ionization and to $v/c = 0.68$ by using spin-polarized muons. The angular precession of the spin of μ^+ particles which traversed magnetized-iron plates and stopped in aluminum was measured. Decay positrons were detected at 0°, 90°, and 270°. Relative phases of the corresponding muon-spin-rotation spectra were obtained as a function of the magnetization direction in the iron. After subtracting the phase shift resulting from the saturation magnetization in the iron and the fringing fields, the experimental result for the dynamic field $\Delta B = -0.5 \pm 2.6$ kG is obtained, in agreement with theoretical expectations for very fast totally stripped ions.

INTRODUCTION

The existence of an intense transient magnetic field acting on fast ions slowing down in magnetic media was discovered in 1968 by Borchers *et al.*[1] The transient field was theoretically described by Lindhard and Winther[2] in 1971 in terms of scattering of polarized electrons in the ferromagnetic medium by the moving ions. Hubler *et al.*[3] in 1974 parametrized the Lindhard and Winther model using existing data for medium-weight ions of low initial velocity, $v/c \lesssim 0.01$. In this model, the field varies inversely with the ion's velocity for $v/c \gtrsim 0.004$, is constant at lower velocity ($0.0005 \lesssim v/c \lesssim 0.004$) and vanishes at low velocity.

In recent measurements[4-10] on faster ions, a dynamic field much larger than that predicted by the adjusted Lindhard-Winther theory[3] was observed and, within the velocity range studied, the field increases with the ion's velocity through the medium. This field was qualitatively described in terms of polarized-electron capture into electron vacancies produced in the moving ion.[8] A recent review of the subject has been given by van Middelkoop.[11]

Experiments have been carried out at the Rutgers-Bell tandem accelerator on ^{56}Fe, ^{82}Se, ^{106}Pd, and ^{112}Cd ions in iron and on ^{82}Se ions in gadolinium in the velocity range $0.01 \lesssim v/c \lesssim 0.05$. In these experiments, the ions were excited to their 2^+ state by a beam of 72-MeV $^{32}S^{8+}$ ions, recoiled through the ferromagnetic foil and stopped in a copper backing where they decayed in an environment free of perturbations. The precession of the angular correlation of the deexcitation γ rays was measured as a function of the direction of polarization of the ferromagnetic material. As the g factor of these states was known, the velocity and Z dependence of the magnetic field was determined. The results obtained with the heavier ions show unambiguously that the dynamic field which acts on the ions studied *increases* with the velocity of the ion. The observed dynamic field has been phenomenologically described by a function of the velocity and atomic number of the ion[5,8]:

$$B(Z, v) = aZ^{3/2}(v/v_0)\mu_B N_p , \tag{1}$$

where $v_0 = e^2/\hbar$, N_p is the polarized-electron density and μ_B is the Bohr magneton. For iron $\mu_B N_p = 1752$ Oe and $a = 12 \pm 0.5$.

An alternate parametrization in terms of the effective charge of the ion passing through the magnetic material fits the data equally well:

$$B(z, v) = a' Z_{\text{eff}}^{3/2} \mu_B N_p , \tag{2}$$

where

$$Z_{\text{eff}} = Z[1 - \exp(-v/v_0 Z^{0.54})] \tag{3}$$

is the best fit to the observed effective charge of ions leaving a solid foil,[12] and $a' = 140 \pm 8$.

In both parameterizations, the field depends on the type of ferromagnet only through the number of polarized electrons per unit volume, suggesting that atomic shell or band-structure effects may not play a significant role for heavier ions.

As the nature of the dynamic field—a hyperfine interaction between the partially stripped ion and the magnetized medium—is not yet fully understood, it is not at all evident that the parametrization of the field which seems to fit the data in the velocity range $0.01 \lesssim v/c \lesssim 0.05$, should extend to higher velocity. At velocities greater than Zv_0, where the ions are completely stripped, the solid can probably be treated as a gas of polarized electrons and a dynamic magnetic field inversely proportional to the ion velocity should result.[2,13]

In order to test the validity of the charge and velocity dependence of the alternate parametrizations, high velocity, totally stripped ions should be used. For this purpose, the effect of the dynamic field on polarized positive muons traversing a thin magnetized iron plate was investigated.

Previous studies using the spin precession of muons stopped in unmagnetized iron have found that the field is 3.6 kG at room temperature, for a sample in zero external field.[14,15] This field is explained in terms of a dipolar contribution from the iron ions and a contact interaction with the polarized screening electrons.[16] These results imply that the dynamic field on the muon is not very large. Otherwise the residual polarization of the muon's spin would have been lost on traversing the unmagnetized iron, washing out the spin precession signal of the stopped muon.[15]

In the present experiment, the effects on muons which traverse a magnetized iron plate and subsequently stop in an aluminum target located in a fixed externally applied magnetic field were observed. The angle through which the spin has precessed in the iron is detected as a phase shift in the oscillatory μSR (muon spin rotation) spectra of the stopped μ^+.[17]

EXPERIMENTAL PROCEDURE

The experiment was carried out with the apparatus shown schematically in Fig. 1. Positive pions are produced at an internal target in the SREL (Space Radiation Effects Laboratory) synchrocyclotron[18] and focused into an external meson channel. The momentum analyzing magnet M is adjusted to select μ^+ particles which originate from π^+ decays in the backwards direction in the π^+ frame of reference. The π^+ decays produce a beam of spin polarized muons, a well-known consequence of parity nonconservation in weak interactions. The arrangement of charged particle scintillation detectors is also shown in Fig. 1. Figure 2 shows the measured particle flux at detector A as a function of momentum, as determined by varying the current through the deflecting magnet M. The μ^+ beam passes through a magnetized Fe plate in the reversible magnet $C1$, and stops in an Al target located in a constant magnetic field produced by magnet $C2$.

The logic coincidence $AB\overline{F}$ establishes that a μ^+ stopped in the target. The mean momentum of the incident μ^+ beam, 103 MeV/c, was deduced from the range measurements shown in Fig. 3, using the known momentum dependence of the muon's range in various materials.[19] The mean kinetic energy of the incident beam is 42 MeV and the

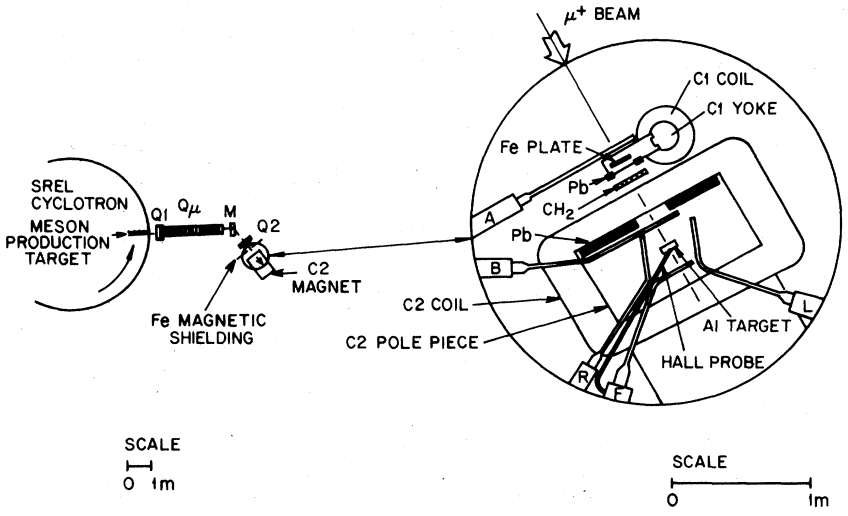

FIG. 1. Layout of the meson channel at SREL and the μSR apparatus in the target area. $Q1$ and $Q2$ are input and output quadrupole magnets, $Q\mu$ the "drift tube" where the pions decay into muons, and M the momentum selection magnet. The gap of magnet $C2$ is 30 cm. The Al stopping target is located 50 cm downstream from the Fe plate.

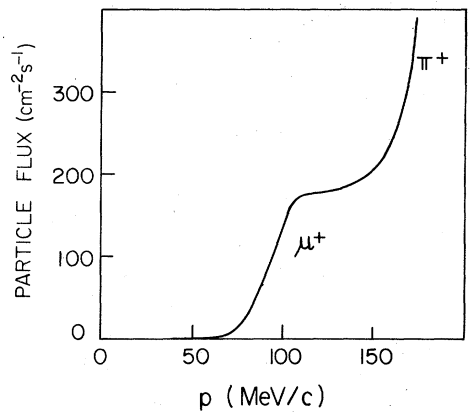

FIG. 2. Total particle flux at the output of the meson channel. The *M* magnet current settings have been converted to an approximate momentum scale. The shoulder at 100 MeV/*c* results from the backwards decay muons. The pion peak occurs at about 230 MeV/*c*.

mean velocity is 0.68*c*. Two range curves are shown, for the aluminum stopping target used for the phase-shift measurement, and the other for a thinner Cu target. The width of the momentum distribution is determined more accurately with the Cu target. The momentum spread is about ±8 MeV/*c*, corresponding to a velocity spread of ±0.03*c*. The experiment was carried out separately for different Fe plates of thicknesses varying from 0.1 to 0.8 cm inserted in the *C*1 magnet. The mean velocity of the muons in the Fe was decreased by up to 6%. The energy of the muon beam hitting the target was kept approximately constant by adding appropriate amounts of CH_2 degrader to compensate for the thinner Fe plates.

The iron plates were fabricated from 99.99% Fe, machined into sheets 12.7-cm square and 0.05- to

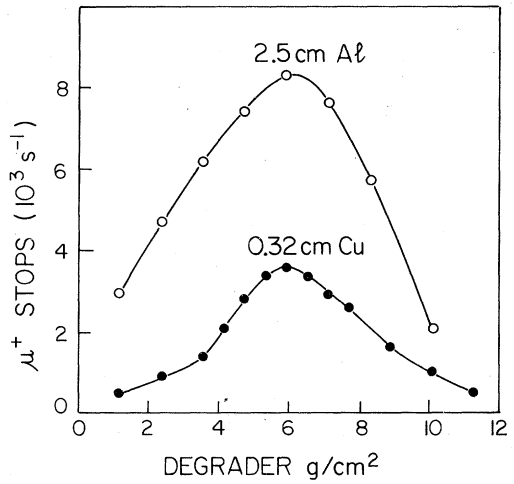

FIG. 3. Muon stopping rate in Al and Cu targets vs thickness of CH_2 degrader placed in front of the target.

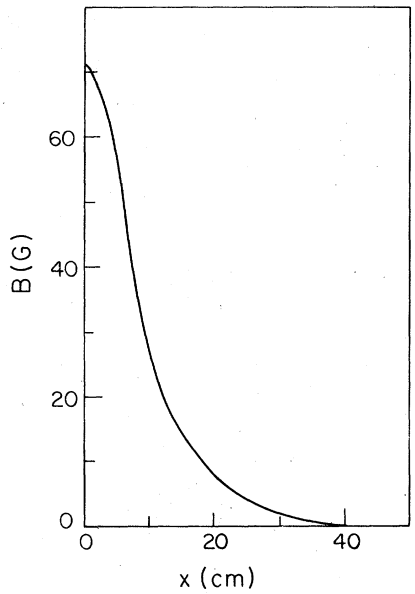

FIG. 4. Axial variation of the vertical component of the field produced by the *C*1 magnet along the beam direction.

0.04-cm thick and subsequently annealed. The electromagnet *C*1 has a movable iron yoke that mates evenly against the edges of the plates. The direction of the magnetization of the Fe plate is vertical. The magnetic induction in the plate was measured by integrating the voltage produced in a sense coil wound around the plate as the *C*1 magnet is energized. For 1600 ampere-turns a magnetic induction of 16 kG is produced in the plate. The profile of the fringing field outside the plate was mapped along the beam axis, and is shown in Fig. 4. The fringing field was insensitive to the Fe plate thickness in the range 0.1–0.8 cm.

The muon beam was collimated to an approximately 12-cm square aperture by the *C*1 magnet yoke and additional 5-cm thick Pb shields placed at each side of the Fe plate. The profile of the μ^+ beam at the Al target position (Fig. 5) was scanned horizontally in the direction transverse to the beam, for the two directions of magnetization of the Fe plate with a 2.5-cm square scintillation detector. These measurements show a bending of the beam, due mainly to the deflection in the magnetization field in the Fe plates and to a lesser extent to the fringing field. For an Fe plate of thickness d_{Fe} a bending angle φ_B may be calculated from the measured magnetization and fringing fields:

$$\varphi_B = (0.067\ \text{cm}^{-1}) d_{Fe} + 0.006 . \quad (4)$$

The aluminum target was 5-cm wide by 10-cm high and 2.5-cm thick. The local field at the tar-

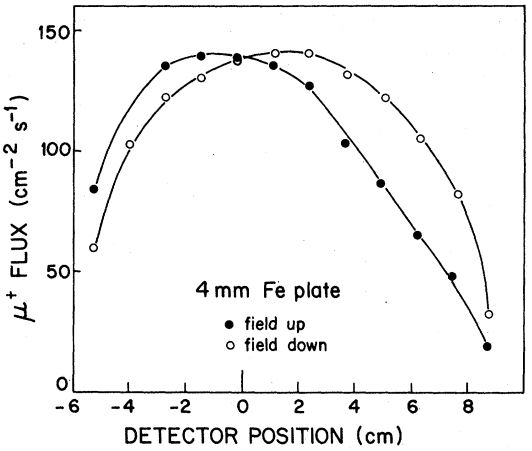

FIG. 5. Scans of the muon beam intensity, taken with a 2.5-cm square detector located at the Al target position and moved along the horizontal transverse direction. "up" and "down" refer to the direction of the magnetization of the Fe plate.

get was 105 Oe. Magnetic shims were positioned near the pole tips of $C2$ in order to produce a homogeneous field at the target. The root-mean-square variation in the field was 0.1 G over the target volume, with the $C1$ magnet off. Maps of the local-field distribution were also made when $C1$ was turned on, for both polarities of the $C1$ current. A small nonlinear variation in the field was found in the horizontal plane, which resulted in a 0.03-G shift of the average field with respect to the field at the center of the target. This field was held constant by adding an extra coil on the $C2$ magnet which was energized by a feedback signal from a Hall-effect probe inserted into a 0.6-cm hole drilled to the center of the target. The field at the center of the target varied by less than 0.01 G as the $C1$ current was reversed.

Positron decays in the 0°, 90°, and 270° directions with respect to the beam direction were detected by the scintillators F, L, and R shown in Fig. 1. At a time t after the μ^+ stops in the target, a positron decay event in one of the three directions is indicated by the logic coincidence $F\bar{A}\bar{B}$, $L\bar{A}\bar{B}$, or $R\bar{A}\bar{B}$, respectively. Six spectra of events versus time were recorded in a multichannel analyzer corresponding to the three positron detectors and the two directions of the Fe magnetization. The total event rate after μ^+ and e^+ pile-up rejection was about 10^3 sec^{-1}. The direction of $C1$ was reversed, and the data acquisition was momentarily disabled, after each increment of 2×10^5 events. The data acquisition system included a magnet controller, actuated by a presettable scaler, and a PDP 11/10 computer. The muon stop and event rates were continuously monitored. The true zero of time was periodically recorded by detecting prompt signals associated with scattered muons. The timing calibration of the analyzer was also checked before and after each run. A low magnetic field in $C2$ is desirable since spurious phase shifts originating from electronic timing drifts increase in proportion to the spin precession frequency.

Several runs were carried out on each of a variety of Fe plates 0.1-, 0.4-, 0.6-, and 0.8-cm thick, respectively. The spectra corresponding to either of the three detectors at 0°, 90°, or 270° were fitted using a nonlinear least-squares method[20] with the following model μSR function:

$$N(t)=A_\pm e^{-t/\tau}\{1+a_\pm e^{-\lambda t}\cos[(\omega\pm\Delta\omega)t + \varphi\pm\Delta\varphi]\}+B_\pm\,, \qquad (5)$$

where (+) or (−) applies to the spectra for the two directions of Fe plate magnetization. The fitting procedure treats A_+, A_-, a_+, a_-, λ, ω, $\Delta\omega$, φ, $\Delta\varphi$, B_+, and B_- as 11 adjustable parameters. The muon lifetime $\tau=2.1994$ μsec is used.

The parameters $a_\pm$ give the magnitude of the asymmetry, which depends upon geometrical details such as the polarization of the muon beam and the selectivity in the e^+ detection. These effects are illustrated in Fig. 6, where the asymmetry measured for a thin Cu target is shown as a function of the incident μ^+ momentum as determined by the thickness of the degrader interposed in the beam. The results display the dependence of the asymmetry upon the average momentum of the stopped μ^+ and the target thickness, which affect the energy of the emitted e^+. The angle φ is an average geometric angle determined by the average initial spin orientation of the μ^+ beam and the location of the positron detector. The angular precession frequency of the stopped muons is $\omega=\gamma_\mu\times105$ G $=9.0\times10^6$ sec^{-1}. The factor $\exp(-\lambda t)$ takes into account the inhomogeneity in the local field in the target.

The phase-shift parameter $\Delta\varphi$ gives the change

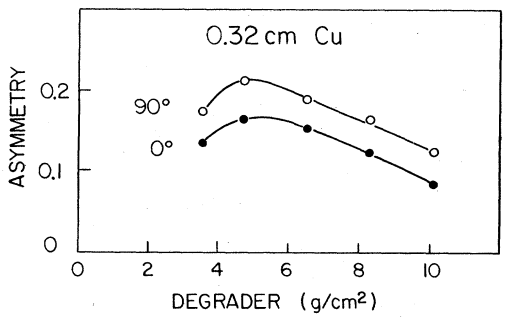

FIG. 6. Positron decay asymmetry measured as a function of the CH_2 degrader thickness.

TABLE I. Fitted parameters for the 0.4-cm thick Fe plate, according to Eq. (5). Statistical errors in the least significant figures are given in parentheses.

	0°	90°	270°
Events	1.1×10^7	1.7×10^7	1.5×10^7
a_+	0.140(1)	0.169(1)	0.157(1)
a_-	0.140(1)	0.173(1)	0.154(1)
$\lambda(10^4\ \mathrm{sec}^{-1})$	4.0(3)	4.6(3)	3.9(3)
$\omega(10^6\ \mathrm{sec}^{-1})$	8.979(4)	8.957(3)	8.958(3)
$\Delta\omega(10^6\ \mathrm{sec}^{-1})$	0.002(4)	−0.001(3)	−0.008(3)
φ	−0.316(8)	−1.801(8)	1.145(8)
$\Delta\varphi$	0.021(9)	0.021(7)	0.034(8)

in the spin orientation of the muon beam produced by the magnetization and dynamic fields in the Fe plate and the fringing field. Both the magnitude and the statistical uncertainty in $\Delta\varphi$ are insensitive to the sampling time interval of the multichannel analyzer and to the magnitude of the field on the Al target. This result was deduced from the analysis of model simulations of the experiment. The parameter $\Delta\omega$ was included in the model function in order to account for a possible small change in local field when $C1$ is reversed. The parameter $\Delta\varphi$ is strongly correlated with $\Delta\omega$, the correlation coefficient being 0.8. The correlation coefficients between $\Delta\varphi$ and the other parameters have magnitudes less than 0.1. Typical values obtained for the 0.4-cm Fe plate are given in Table I, while the phase shifts obtained for the other thicknesses of Fe are displayed in Table II.

An alternate procedure was also tested, whereby $\Delta\omega$ was set to 0 and 10 adjustable parameters were varied. This analysis did not produce statistically significant changes in $\Delta\varphi$, although the statistical errors in $\Delta\varphi$ were reduced by 40%. In the 11-parameter fits, the $\Delta\omega$ values were smaller than the statistical errors in $\Delta\omega$.

DISCUSSION OF THE RESULTS

As the muon velocity in the iron is approximately constant, the phase shift is proportional to the time spent in the iron plate and hence varies linearly with the thickness of the plate:

$$\Delta\varphi = r d_{\mathrm{Fe}} + \Delta\varphi_0 . \tag{6}$$

The slope r and the intercept $\Delta\varphi_0$ were obtained from a linear least-squares fit and are given in Table III. The results for the 11-parameter fitting procedure appear to be more consistent, and were adopted as the better representation of the results. There does not appear to be a systematic influence of the beam bending, since the three detectors give the same precession angle within the statistical error. The geometric effect caused by the lateral deflection of the beam was expected to be maximum for the 0° detector, where it would tend to increase $\Delta\varphi$. The width of the Al target was chosen to be narrow compared to the width of the muon beam, in order to minimize this effect. The magnitude of the beam bending influence was estimated in a model calculation where beam profiles such as the typical one shown in Fig. 5 were assumed to represent the spatial distribution of stopped muons in the target. The calculation neglected positron scattering and attenuation in the target and a small inhomogeneity known to exist in the efficiency of the scintillator. The calculation gives a geometric contribution to the phase-shift parameter r of 0.001 cm^{-1}, which is near the limit of detection.

The net precession angle averaged over the three detectors is plotted against the Fe plate thickness in Fig. 7. The solid line represents the linear least-squares fit. From the slope $r = 0.065 \pm 0.011$ cm^{-1} of the fitted line and the average muon velocity of $v = 0.68c$, the net field on the muon is ob-

TABLE II. Experimental phase shifts $\Delta\varphi$ obtained for the various thicknesses of Fe plate.

	$\Delta\varphi$(mrad)		
d_{Fe} (cm)	0°	90°	270°
0.1	8(11)	−1(9)	9(10)
0.4	21(9)	21(7)	34(8)
0.6	41(12)	23(10)	32(12)
0.8	49(11)	49(10)	59(11)

TABLE III. Results of fitting the μSR phase-shift measurement of $\Delta\varphi$ to the linear relation given in Eq. (6). The slope r is given in milliradians/cm and the intercept $\Delta\varphi_0$ in milliradians.

Method	Parameters	0°	90°	270°	Average
$\Delta\omega$ variable	r	64(20)	65(18)	65(20)	65(11)
$\Delta\omega$ variable	$\Delta\varphi_0$	−2(11)	−7(9)	4(10)	−1(6)
$\Delta\omega = 0$	r	51(13)	63(12)	55(12)	56(7)
$\Delta\omega = 0$	$\Delta\varphi_0$	5(7)	−5(6)	1(6)	0(4)

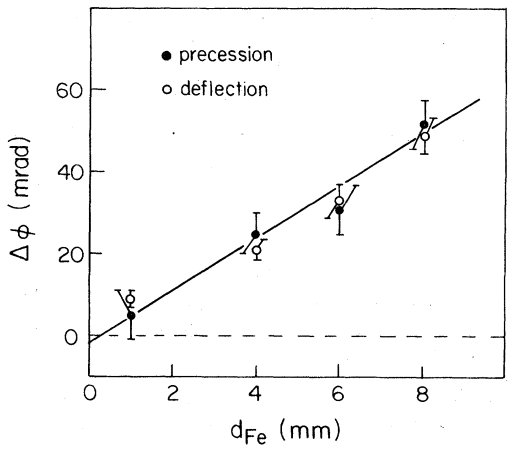

FIG. 7. Muon spin precession angle (phase shift in the μSR fits, open circles) averaged over the three spectra as a function of the thickness of the Fe plate. The least-squares fit (solid line) and the measurements of the beam deflection angles (filled circles) are also shown.

tained:

$$B = rv/\gamma_\mu = 15.5 \pm 2.6 \text{ kG}.$$

Since the stauration field in the Fe plates used was 16.0 kG, the dynamic field enhancement is

$$\Delta B = -0.5 \pm 2.6 \text{ kG}.$$

Thus the observed precession can be explained entirely in terms of the magnetization field. If this result were precisely true, and since $g \approx 2$ for the muon, the beam deflection and spin precession angles must be equal. For comparison, the beam deflection angles calculated from plots such as the one shown for the 0.4-cm plate in Fig. 5 have also been plotted in Fig. 7. These results are consistent with $\Delta B \approx 0$.

In Table IV the values for ΔB resulting from the parametrizations of the dynamic field obtained from heavy-ion reactions, and from the theoretical calculations of Sak and Bruno are listed. If the extrapolation based upon Eq. (1) were applicable

TABLE IV. Calculation of the dynamic field and ensuing total phase shifts $\Delta\varphi$ for muons at $v/c = 0.68$, or $v/v_0 Z = 93$, based on three proposed parametrizations of the dynamic field. The saturation field of the iron was taken as 16 kG, the measured value for the iron plates used in the experiment.

	ΔB (kG)	$\Delta\varphi/d_{Fe}$ (cm^{-1})
Dynamic field Eq. (1)	1530	5.96
Dynamic field Eq. (2)	178	0.73
Sak and Bruno Eq. (7)	0.17	0.0063
Experiment	< 2.6	

here, the field would be proportional to the velocity of the muon, and the resulting phase shift would in turn be proportional to the Fe plate thickness d_{Fe}:

$$\Delta\varphi = \int \gamma_\mu B\, dt = \gamma_\mu a Z^{3/2} \mu_B N_p \int \frac{v}{v_0}\frac{dx}{v}$$

$$= \gamma_\mu a Z^{3/2} \mu_B N_p d_{Fe}/v_0 .$$

This phase shift turns out to be $(8.2\ \text{cm}^{-1}) d_{Fe}$ radians—a rather dramatic prediction. The data easily rule out such an extrapolation of the field to high velocity.

Although we do not have a precise measure of the dynamic field, our result is in agreement with the Sak and Bruno prediction[13] for $v \gg v_0 Z$:

$$\Delta B = 4\pi Z \mu_B N_p v_0/v . \tag{7}$$

Lindhard and Winther did not acutally evaluate the enhancement of the magnetic field at high velocity. Their theory was designed to explain the large magnetic fields acting on relatively slow ($v \ll Z v_0$) ions. For this reason, they assume the field is approximately spherically symmetric and neglect the asymmetric corrections represented in their notation by the parameter ξ. These corrections are, however, important at high velocity. Hence the Lindhard-Winther theory is not directly applicable to fast ions or muons. Furthermore, even though in principle their theory could apply to slow ions, they also neglect atomic shell effects and assume that the ions are essentially stripped. Shell effects can be neglected only for swift ions with $v \gg v_0 Z$, hence in just the region where the asymmetry corrections are important.

It would be very interesting to fill in the large gap in velocity between the present muon experiment and the heavy-ion experiments. The two experiments taken together indicate that there is a maximum in the velocity dependence of the dynamic field. However, the possibility exists that the large dynamic field observed with heavy ions may partly be due to atomic effects such as equilibrium between hole production and capture of polarized electrons from the medium. Experiments on very slow muons ($v \lesssim v_0$) and on very fast totally stripped heavy ions ($v \gtrsim Z v_0$) may be necessary for a better understanding of the dynamic field.

In conclusion we mention two examples of related work with positive muons. It is known that the μ^+ picks up a bound electron in semiconductors and insulators, forming a muonium atom. Recently, a muonium stage for μ^+ stopping in a Ge

crystal has been observed through a measurement of the phase shift in the μSR signal associated with muonium precession in a transverse external field.[21] Also, our results show that magnetized solid Fe deflectors and lenses may indeed be used for the transport and focussing of high-energy muon beams without significant loss of polarization.[22]

ACKNOWLEDGMENTS

This work was supported in part by the NSF, the Commonwealth of Virginia, and NASA.

---

*Present address: Weizmann Institute, Rehovot, Israel.

[1]R. R. Borchers, B. Herskind, J. D. Bronson, L. Grodzins, R. Kalish, and D. E. Murnick, Phys. Rev. Lett. 20, 424 (1968).
[2]J. Lindhard and A. Winther, Nucl. Phys. A 166, 413 (1971).
[3]G. K. Hubler, H. W. Kugel, and D. E. Murnick, Phys. Rev. C 9, 1954 (1974).
[4]M. Hass, J. M. Brennan, H. T. King, T. K. Saylor, and R. Kalish, Phys. Rev. C 14, 2119 (1976).
[5]J. M. Brennan, N. Benczer-Koller, M. Hass, and H. T. King, Hyperfine Interactions 4, 268 (1978).
[6]N. Benczer-Koller, M. Hass, J. M. Brennan, and H. T. King, J. Phys. Soc. Jpn. 44, 341 (1978).
[7]J. L. Eberhardt, G. Van Middelkoop, R. E. Horstman, and H. A. Doubt, Phys. Lett. B 56, 329 (1975).
[8]J. L. Eberhardt, R. E. Horstman, P.C. Zalm, H. A. Doubt, and G. Van Middelkoop, Hyperfine Interactions 3, 195 (1977).
[9]M. Forterre, J. Gerber, J. P. Vivien, M. B. Goldberg, K.-H. Speidel, and P. N. Tandon, Phys. Lett. B 55, 56 (1975).
[10]C. Fahlander, K. Johansson, E. Karlsson, and G. Possnert, Hyperfine Interactions 4, 278 (1978).
[11]G. van Middelkoop, Hyperfine Interactions 4, 238 (1978).
[12]H. D. Betz, Rev. Mod. Phys. 44, 465 (1972).
[13]J. Sak and J. Bruno (private communication).
[14]M. L. G. Foy, N. Heiman, W. J. Kossler, and C. E. Stronach, Phys. Rev. Lett. 30, 1064 (1973).
[15]I. I. Gurevich, A. I. Klimov, V. N. Maiorov, E. A. Meleshko, B. A. Nikol'skii, V. I. Selivanov, and V. A. Suetin, Zh. Eksp. Teor. Fiz. 69, 439 (1975). [Sov. Phys. -JETP 42, 222 (1976)].
[16]P. F. Meier, Solid State Commun. 17, 987 (1975).
[17]For a review of the μ SR technique, see A. Schenck, *Nuclear and Particle Physics at Intermediate Energies*, edited by J. B. Warren (Plenum, New York, 1975). p. 176.
[18]The Space Radiation Effects Laboratory, Newport News, Virginia 23606. A description of an earlier version of the SREL meson channel has been given by H. O. Funsten, Nucl. Instrum. Methods 94, 443 (1971).
[19]Lawrence Berkeley Laboratory Report No. UCRL-2426, 1966, revised (unpublished).
[20]D. W. Marquardt, J. Soc. Indust. Appl. Math. 11, 431 (1963).
[21]V. I. Kudinov, E. V. Minaichev, G. G. Myasischeva, Yu. V. Obukhov, V. S. Roganov, G. I. Savel'ev, V. M. Samoilov, and V. G. Firsov, Pis'ma Zh. Eksp. Teor. Fiz. 21, 49 (1975) [JETP Lett. 21, 22 (1975)].
[22]J. Lebritton, F. Lobkowicz, S. C. Melissinos, and W. Metcalf, Nucl. Instrum. Methods 141, 81 (1977).